ChemCatChem

The European Society Journal for Catalysis

Chemistry Europe

European Chemical Societies Publishing

Supported by GECATS GERMAN CATALYSIS SOCIETY

Accepted Article

Title: Engineering a carbonyl reductase as a potential tool for the synthesis of chiral α-tetralinols

Authors: Aipeng Li, Ting Wang, Ke Yang, Xuanshuo Zhang, Dongming Yin, Yong Qin, and Lianbing Zhang

To be cited as: *ChemCatChem* 10.1002/cctc.202100890

Link to VoR: https://doi.org/10.1002/cctc.202100890

WILEY-VCH

10.1002/cctc.202100890

WILEY-VCH

FULL PAPER

Engineering a carbonyl reductase as a potential tool for the synthesis of chiral α-tetralinols

Aipeng Li,[a] Wang Ting,[a] Ke Yang,[a] Xuanshuo Zhang,[a] Dongming Yin,[a] Yong Qin,*[a, b] and Lianbing Zhang*[a]

[a] Dr. Aipeng Li, Wang Ting, Ke Yang, Xuanshuo Zhang, Dongming Yin, Prof. Yong Qin, Prof. Lianbing Zhang
School of Life Sciences
Northwestern Polytechnical University
710072 Xi'an, China
E-mail: lbzhang@nwpu.edu.cn

[b] Prof. Yong Qin
State Key Laboratory of Coal Conversion, Institute of Coal Chemistry
Chinese Academy of Sciences
030001 Taiyuan, China
E-mail: qinyong@sxicc.ac.cn

Supporting information for this article is given via a link at the end of the document.

Abstract: Tailoring of enzyme toward α-tetralones, a class of bulky-bulky ketones, is still a challenge. In this work, the mutants of carbonyl reductase BaSDR1 with improved catalytic performance toward α-tetralone **1a** were obtained by adjusting the steric hindrance and hydrophobicity of the residues that affect the approach of α-tetralone with the catalytic residues. The designed mutants also showed enhanced catalytic performance toward halogenated α-tetralones **2a**-**6a**. Remarkably, the activity of the mutant Q237V/I291F toward 7-fluoro-α-tetralone **5a** was 16.3-fold higher than the wildtype enzyme with improved stereoselectivity (98.8% ee). More notably, the mutants Q139S and Q139S/V187S exhibited decreased or reversed stereoselectivity toward α-tetralone **1a**, 5-bromo-α-tetralone **2a**, 7-fluoro-α-tetralone **5a** and 7-chloro-α-tetralone **6a**, while the relatively high ee values were obtained in the presence of 6-chloro-α-tetralone **3a** and 6-bromo-α-tetralone **4a** as substrates. Further analysis showed the larger size of the substrates was beneficial for the substrates binding to the active cavity with a more specific binding mode, which endows the reaction with higher stereoselectivity. Moreover, the recombinant *E. coli* expressing the variant Q237V/I291F successfully catalyzed the reduction of a high concentration 7-fluoro-α-tetralone **5a**. These results not only offered a potential tool for chiral α-tetralols, but also provided guiding information for the enzyme engineering toward bulky-bulky ketones.

Introduction

Chiral α-tetralol and its halogenated derivatives are important chiral scaffolds for the synthesis of pharmaceuticals. For instance, enantiomerically pure α-tetralol is a versatile intermediate to access sulfonamide compounds having TRPM8 antagonistic activity,[1] inhibitors for treating central nervous system disorders,[2] ORL-1 receptor agonist [3] and antidepressant;[4] (*S*)-7-Fluoro-α-tetralol is used to synthesize purinone derivatives, which are useful for indications such as leukemias and lymphomas, organ and bone marrow transplant rejection, mast cell-mediated allergic reactions and inflammatory diseases.[5] Thus, considerable efforts have been devoted to the synthesis of optically active α-tetralols.

Enzyme-mediated asymmetric reduction is a preferable technology due to its mild reaction conditions and environmental friendliness.[6] Several biocatalytic approaches have been reported for the preparation of chiral α-tetralol.[7] However, the biocatalytic asymmetric reduction is still far from feasible for the preparation of chiral α-tetralol due to their insufficient catalytic activity, unsatisfactory stereoselectivity or low substrate loading. Moreover, previous studies mainly focused on the asymmetric reduction of α-tetralone, specific biocatalysts for the reduction of halogenated α-tetralones were seldom reported. The lack of specific biocatalysts cannot satisfy the demand for the halogenated chiral α-tetralols. Given the importance of chiral α-tetralol and its halogenated derivatives in the synthesis of bioactive molecules, it is necessary to develop enzymes with robust capacity for the production of chiral α-tetralols.

Engineering of existing protein provides a convenient way to create desired enzymes toward given substrates.[8] In particular, rational design has been demonstrated as an effective strategy to adjust enzyme catalytic performance, including activity improvement,[9] stereoselectivity modification,[10] stability enhancement [11] and substrate scope expansion.[12] Nevertheless, rational engineering of enzymes for the asymmetric reduction of bulky-bulky ketones, which bear two bulky substituents, is still a major challenge.[13] As precursors for the asymmetric synthesis of chiral α-tetralols, α-tetralones belong to the class of bulky-bulky ketones. The elusive effect of the structure of the bulky-bulky ketones, such as the substrate size and the presence of substituent group, on the enzyme catalytic performance was the main reason that hampers the obtaining of ideal enzymes by rational design. Besides, the carbonyl group of α-tetralones is located closer to the aromatic ring compare with their counterparts such as β-tetralones. The large steric hindrance and unique properties of aromatic ring might make the contact of the catalytic residues of the enzyme with the carbonyl group of the substrates more difficult, which impedes enzymatic performance. Moreover, it was reported that the minor differences in the substrate structure might exert great influence on the binding of the ligand and the protein receptor, leading to the obviously different enzyme activity and stereoselectivity.[14] Therefore, it is more challenging to tailor specific enzyme toward the asymmetric reduction of α-

tetralone and its halogenated derivatives. An in-depth understanding of the effect of the substrate structure on the enzyme catalytic performance is of great fundamental importance in the rational design of the specific enzyme.

In our previous study, a carbonyl reductase (BaSDR1) from Bacillus aryabhattai was discovered to be an excellent biocatalyst for the reduction of aromatic ketones, especially *ortho*-haloacetophenones.[15] However, the wildtype BaSDR1 showed poor activity toward α-tetralone **1a** (Scheme 1 and Table 1). Herein, to obtain robust enzyme for the synthesis of chiral α-tetralols, the reconstruction of the catalytic pocket of carbonyl reductase BaSDR1 was performed by rational adjusting the steric hindrance and hydrophobicity of the residues that affect the approach of α-tetralone **1a** with catalytic active site. The mutants with significantly enhanced catalytic activity and high stereoselectivity toward α-tetralone **1a** were obtained. Then, the stereoselectivity and activity of the designed mutants toward halogenated α-tetralones (**2a**-**6a**), which bear various size halogen atom at different position of the aromatic ring, was evaluated to further clarify the effect of the structure of the bulky-bulky ketones on enzyme catalytic performance. Furthermore, the mechanism behind the changed catalytic performance was analysed. And the effect of the structure of the bulky-bulky ketones on enzyme catalytic performance, especially stereoselectivity, was emphatically discussed. Finally, the whole cell catalyzed synthesis of optical pure (*S*)-7-fluoro-α-tetralol, which is an important building block for the synthesis of chiral pharmaceuticals,[5] was presented as an example to demonstrate the application potential of the designed mutants in the production of chiral α-tetralols.

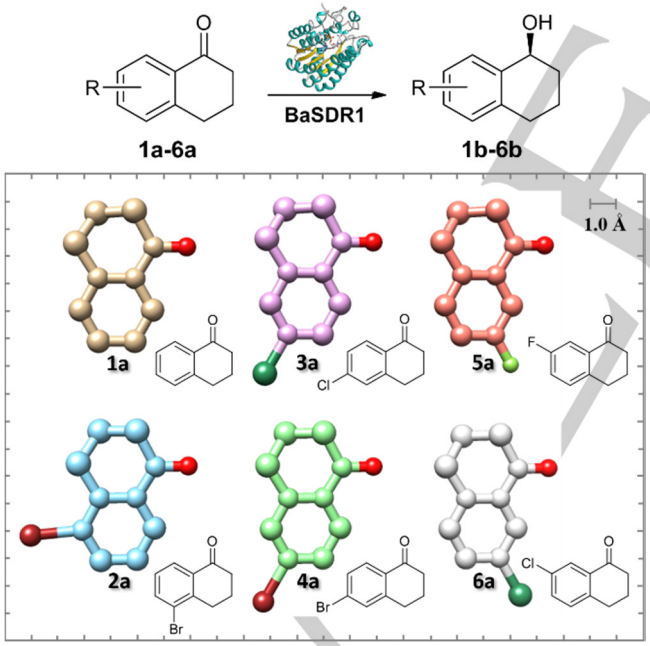

Scheme 1. Asymmetric reduction of α-tetralones to the corresponding chiral alcohols by BaSDR1.

Results and Discussion

Rational design of BaSDR1 for asymmetric reduction of α-tetralone

To clarify the molecular basis behind the low catalytic activity of BaSDR1 toward α-tetralone **1a** and identify the targets for protein engineering, the substrate **1a** was docked into the catalytic pocket of BaSDR1 (Figure 1). Substrate **1a** showed two typical binding modes in the catalytic cavity. In one binding mode, the aromatic ring and the cyclohexane ring of the substrate **1a** were vertical to the bottom of the substrate-binding pocket (Figure 1c), while these groups were almost parallel to the bottom of the substrate-binding pocket in the other binding mode (Figure 1d). These substrate binding modes shared some similarities. The cyclohexane ring of substrate **1a** directed to residues Q139, Q237 and F250, while its aromatic ring was oriented toward residues V187 and I291. Such orientation ensures that NADH delivers its hydride to *Re*-face of the substrate **1a**, leading to the formation of the corresponding (*S*)-alcohols. The docking results are in good agreement with the experimental observations (Table 1 and Table 2).

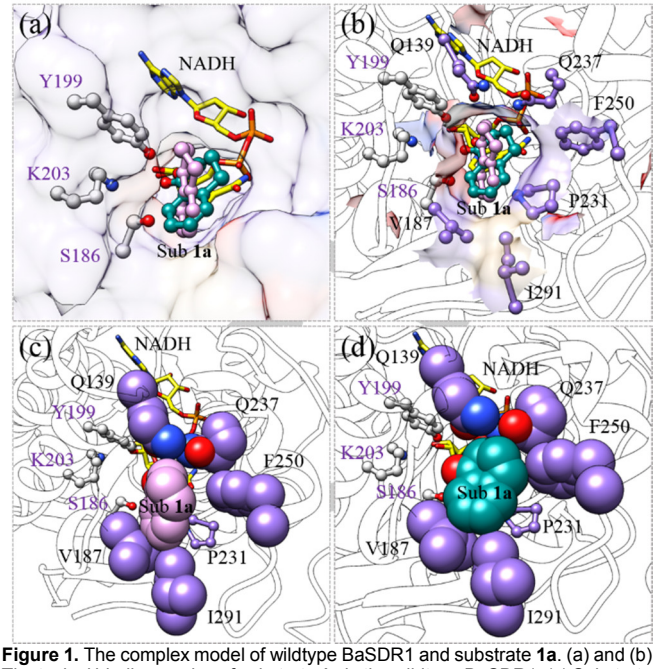

Figure 1. The complex model of wildtype BaSDR1 and substrate **1a**. (a) and (b) The typical binding modes of substrate **1a** in the wildtype BaSDR1; (c) Substrate **1a** with vertical binding pose in the active site; (d) Substrate **1a** with parallel binding pose in the active site.

It is noteworthy that the catalytic pocket space seems too small to give enough steric flexibility for the bulky-bulky ketone **1a**. There are only narrow spaces between substrate **1a** and the residues Q139, V187, Q237, F250 and I291 (Figure 1c and 1d). It might hamper the effective contact of the catalytic residues of the enzyme with the carbonyl group of the substrates and further caused the low catalytic activity of BaSDR1 toward α-tetralones. Moreover, the limited structural flexibility and the relatively large size of α-tetralone makes it difficult for the substrates to adjust their structure spontaneously to gain a more productive binding pose. To provide a suitable catalytic pocket for α-tetralone binding, the residues Q139, V187, Q237, F250 and I291, which closely adjacent to the substrate, were selected as the engineering targets and re-designed.

As shown in Figure 1, the residues Q139, Q237 and F250 are located on the side of the substrate cyclohexane ring and carbonyl group. Obviously, the bulky side chain of these three residues blocked the approach of the catalytic residue Y199 with the carbonyl group of the substrate. Thus, Q139, Q237 and F250 were replaced by residues harboring a relatively small side chain such as alanine, glycine, valine, leucine, serine, aspartate and

asparagine. Moreover, previous study indicated that the proximity of substrate to the catalytic residues could be driven by the change of the side chain property or the increased steric hindrance of residue in a special position.[15-16] The residues V187 and I291 positioned on the other side of the catalytic residue Y199. Thus, the change of the side chain property or increased steric hindrance of these two residues might be a feasible strategy for pushing the substrates close to the catalytic residues and further enhancing the catalytic activity. Therefore, similar size residues with different property (charge property and hydrophobicity of the amino acid side chain) or residues with a bulky side chain were introduced at those sites. Based on the above analysis and design, a series of single-mutation variants were generated by site-directed mutagenesis.

Asymmetric reduction of α-tetralones

The designed mutants were used to catalyze the asymmetric reduction of α-tetralone **1a** for evaluation of their catalytic performance. As shown in Table 1 and Table S1, three variants based on residue Q139 (Q139S, Q139G and Q139A) exhibited significantly enhanced specific activities. Particularly, the variant Q139S displayed the highest improvement among those of all the variants tested, the specific activity enhanced from 21.25 to 170.37 mU/mg toward substrate **1a**, an 8.02-fold enhancement. However, the trade-off between activity and stereoselectivity was observed when Q139 was substituted. The mutants Q139S and Q139G exhibited reversed enantiomeric preference towards substrate **1a**, while the stereoselectivity of the mutants Q139A, Q139L, Q139I, Q139V, Q139T and Q139C was obviously decreased as compared with the wildtype enzyme (Table 1 and Table S1). Moreover, the substitutions at residues V187, Q237 and I291 also exhibited enhanced specific activity. In particular, the mutants V187S, Q237V and I291F possessed the most significant increase in the catalytic activity compared with other mutants at corresponding sites, respectively. More importantly, none of the variants based on residue V187 and Q237 caused an adverse effect on stereoselectivity, though the mutation at residue I291 slightly decreased the enzyme stereoselectivity (Table 1).

Furthermore, the combination of these single-mutations was performed to investigate whether there would be a synergic effect or not. As shown in Table 1 and Table S1, compared with the corresponding single-point mutants, further increased activity was observed when the mutant Q237V/I291F was utilized as catalyst, reaching the specific activity values up to 94.26 mU/mg. Though the variants Q139S/V187S and Q139G/V187S exhibited a lower activity compared with their single mutant counterparts Q139S and Q139G, respectively, both of them had significant improvement compared with the wildtype BaSDR1 and the mutant V187S. The specific activity of the other double-point mutants was lower than that of the corresponding single point mutants. Based on above results, though the mutants Q139S and Q139S/V187S exhibited undesired stereoselectivity, their catalytic activity was attractive. Therefore, the mutants Q139S, V187S, Q139S/V187S, Q237V, I291F and Q237V/I291F were selected to further evaluate their catalytic performance toward halogenated α-tetralones (**2a**-**6a**) and investigate the effect of the substrate structure on the enzyme catalytic performance.

As shown in Table 2, the single-mutation variants Q139S exhibited obviously enhanced activity toward all halogenated α-tetralones (**2a**-**6a**), the enhancement of the specific activity varied from 1.9- to 14.6-fold. The designed mutants V187S, Q237V and I291F also improved the catalytic activity toward the majority of halogenated α-tetralones. Exceptionally, the specific activity of the mutant V187S toward substrate **6a** decreased, and the substitution of Q237 with valine lead to the loss of enzymatic activity toward substrate **3a**. Moreover, a synergic effect in the enhancement of the catalytic activity was observed when the variant V187S/I291F was utilized as the catalyst. The specific activity of the variant V187S/I291F was further enhanced toward the majority of the tested substrates compared with the single-point mutants V187S and I291F (Table 2). And the variant V187S/I291F exhibited excellent stereoselectivity, giving corresponding alcohols with high ee values (97.8-99.7%). In addition, the decreased catalytic activity was found in the reduction of substrates **5a** and **6a** by the variant Q139S/V187S, which was similar to its catalytic performance toward substrate **1a**. Nevertheless, the specific activities of the variant Q139S/V187S toward those substrates were still much higher than those of the wildtype BaSDR1. More notably, the variant Q139S/V187S showed excellent stereoselectivity toward substrates **3a** and **4a**,

Table 1. Asymmetric reduction of α-tetralone **1a** by the wildtype BaSDR1 and its variants

Enzyme	Specific activity (mU/mg)	ee (%)
WT	21.25±3.20	98.7 (S)
Q139S	170.37±10.57	29.2 (R)
Q139G	125.20±5.48	16.5 (R)
Q139A	113.47±6.65	10.3 (S)
Q139L	35.68±3.87	90.5 (S)
Q139D	23.63±2.49	98.5 (S)
Q139N	25.25±1.68	97.6 (S)
Q237V	74.60±5.87	98.5 (S)
Q237G	50.21±2.55	98.2 (S)
Q237A	63.25±3.86	97.9 (S)
Q237L	41.23±5.33	98.3 (S)
Q237D	18.25±2.22	98.5 (S)
Q237N	14.36±4.02	98.7 (S)
Q237S	25.66±1.87	98.0 (S)
F250A	12.31±2.65	98.2 (S)
F250I	15.22±3.68	98.6 (S)
F250S	20.05±4.13	98.3 (S)
F250D	18.25±2.20	97.9 (S)
F250N	15.65±3.69	98.3 (S)
V187S	41.84±4.07	96.8 (S)
V187A	32.67±1.89	97.5 (S)
V187D	26.78±3.88	97.9 (S)
V187T	36.23±4.04	98.0 (S)
V187N	22.29±4.21	97.8 (S)
I291F	38.40±3.29	92.7 (S)
I291N	15.22±1.87	93.2 (S)
I291D	16.98±3.47	92.8 (S)
I291S	19.29±1.08	94.2 (S)
I291L	28.21±4.33	92.9 (S)
Q139S/V187S	156.09±11.18	14.4 (S)
Q237V/I291F	94.26±9.56	97.8 (S)
Q139S/Q237V	42.31±1.33	18.0 (S)
Q139S/I291F	40.02±5.12	14.2 (S)
V187S/Q237V	32.94±2.25	98.3 (S)
V187S/I291F	26.64±3.21	97.7 (S)

Table 2. Asymmetric reduction of prochiral α-tetralones by the wildtype BaSDR1 and its variants.

Enzyme	Substrate	Specific activity (mU/mg)	ee (%)	Substrate	Specific activity (mU/mg)	ee (%)
WT		21.25±3.20	98.7 (S)		27.83±3.38	97.5 (S)
Q139S		170.37±10.57	29.2 (R)		125.78±4.25	17.2 (R)
V187S		41.84±4.07	96.8 (S)		44.88±6.57	99.6 (S)
Q139S/V187S	**1a**	156.09±11.18	14.4 (S)	**2a**	134.14±10.74	72.7 (S)
Q237V		74.60±5.87	98.5 (S)		69.83±4.53	99.7 (S)
I291F		38.40±3.29	92.7 (S)		29.31±2.57	99.3 (S)
Q237V/I291F		94.26±9.56	97.8 (S)		86.71±5.80	98.5 (S)
WT		20.31±4.46	97.4 (S)		19.13±1.17	98.2 (S)
Q139S		39.02±3.31	85.6 (S)		53.71±5.68	98.4 (S)
V187S		57.04±2.80	99.4(S)		41.89±4.72	99.2 (S)
Q139S/V187S	**3a**	99.71±6.28	98.8 (S)	**4a**	120.55±8.41	99.8 (S)
Q237V		Nr [a]	/		40.95±4.51	99.5 (S)
I291F		20.05±1.77	98.5 (S)		24.32±0.95	98.1 (S)
Q237V/I291F		Nr	/		83.82±4.45	99.6 (S)
WT		12.90±3.74	70.0 (S)		12.00±3.20	93.6 (S)
Q139S		187.72±7.90	22.6 (R)		70.34±1.14	22.9 (S)
V187S		57.10±3.05	55.8 (S)		10.13±1.50	90.5 (S)
Q139S/V187S	**5a**	171.63±9.54	56.9 (R)	**6a**	45.96±3.92	49.8 (R)
Q237V		54.75±4.48	95.7 (S)		45.32±3.32	96.5 (S)
I291F		33.52±3.54	92.5 (S)		18.30±2.79	95.1 (S)
Q237V/I291F		210.59±7.35	98.8 (S)		86.07±4.49	99.7 (S)

[a] No reaction was observed.

producing corresponding chiral alcohols with 98.8% and 99.8% ee, respectively. Those results indicated that the presence of halogen atoms and their position at the aromatic ring of substrates had significant effects on the catalytic performance of the enzyme.

In order to elucidate the underlying mechanism contributing to the enhanced catalytic activity toward α-tetralones, the kinetic parameters of the double-point mutants and the wildtype enzyme toward α-tetralone **1a** and halogenated α-tetralones (**2a**, **3a** and **5a**) were determined. As shown in Table 3, the variants Q139S/V187S and V187S/I291F exhibited enhanced catalytic efficiency (k_{cat}/K_m) toward all tested substrates. In particular, the k_{cat}/K_m values of these two mutants toward substrate **5a** were 15.5- and 16.8-fold higher than the wildtype enzyme. Moreover, these two variants exhibited lower K_m values toward the majority of the tested substrates. The binding free energy between the enzymes and α-tetralones are in good agreement with the experimentally determined K_m. The binding free energies of the mutant complex models were lower than those of wildtype enzyme for the majority of the tested substrates (Figure S1), indicating the higher affinity of the variants to the substrates than the wildtype enzyme. These results demonstrated that the improved enzyme-substrate affinity was a main driving force for the elevated catalytic efficiency toward these substrates. Specifically, increases in the K_m value was observed with a simultaneous increase in the k_{cat} value for substrates **1a** when the mutant Q139S/V187S was used as a catalyst. This result revealed that the improved catalytic capability of Q139S/V187S toward substrate **1a** was mainly originated from the high degree of productive binding but not from the enhanced enzyme-substrate affinity.[13b, 17] It is obviously different from the determined kinetic parameters of the mutant Q139S/V187S toward halogenated α-tetralones (**2a**, **4a** and **5a**), indicating the halogen substitution at aromatic ring of the substrates result in distinct effects on enzyme-substrate binding.

Table 3. Apparent kinetic parameters of the wildtype BaSDR1 and the variants toward α-tetralones

Enzyme	Sub[a]	k_{cat} (min^{-1})	K_m (mM)	k_{cat}/K_m (min^{-1} mM^{-1})
WT		5.02±0.96	22.11±1.02	0.23±0.03
Q139S/V187S	**1a**	50.02±2.44	48.29±2.24	1.04±0.05
Q237V/I291F		18.03±1.68	21.96±0.83	0.82±0.06
WT		4.56±1.22	79.62±2.07	0.08±0.02
Q139S/V187S	**2a**	16.10±1.53	30.09±2.31	0.54±0.03
Q237V/I291F		8.64±1.08	18.45±1.41	0.47±0.02
WT		28.98±1.20	387.15±5.22	0.07±0.01
Q139S/V187S	**4a**	46.51±1.26	217.26±4.33	0.21±0.07
Q237V/I291F		10.62±0.87	56.32±2.11	0.19±0.04
WT		9.39±1.33	195.64±1.83	0.04±0.02
Q139S/V187S	**5a**	48.45±1.47	77.73±0.98	0.62±0.06
Q237V/I291F		55.33±1.68	82.61±1.39	0.67±0.05

[a] Abbreviation for substrate.

Molecular basis of the desired activity and stereoselectivity

To explore the molecular basis of the enhanced catalytic activity and the changed stereoselectivity from the perspective of the structure-function relationship, docking of α-tetralones (**1a**, **2a**, **4a** and **5a**) into the structural model of the double-mutation variants was performed (Figure 2 and Figure S2-S4). The substrate binding modes in the mutants shared some similarities with those observed in the wildtype enzyme. Similar with one of the typical binding conformation in the wildtype enzyme, the substrates mainly adopted a vertical conformation, namely the aromatic ring and cyclohexane ring of the substrates were vertical to the bottom of the substrate-binding pocket in the complex models of the variant Q139S/V187S and α-tetralones (Figure 2e and Figure S2b-S4b). The dominant substrate-binding modes in the variant V187S/I291F was similar to another typical binding conformation in the wildtype enzyme, in which the aromatic ring and cyclohexane ring of the substrates were almost parallel to the bottom of the substrate-binding pocket (Figure 2f and Figure S2c-S4c). The difference is that the carbonyl moiety of the substrates was positioned closer to the catalytic triad (Ser186-Tyr199-Lys203) in both double-mutation variants than those in the wildtype enzyme. As shown in Figure 3, the distances between the Tyr199 hydroxyl and the oxygen atom of the substrate carbonyl groups in the variants Q139S/V187S and V187S/I291F were shorter than those in wildtype. Furthermore, compared with those in wildtype, the shorter or almost equal distances between the C_4 atom of the nicotinamide ring of NADH and the carbon atom of the substrate carbonyl groups were observed in both

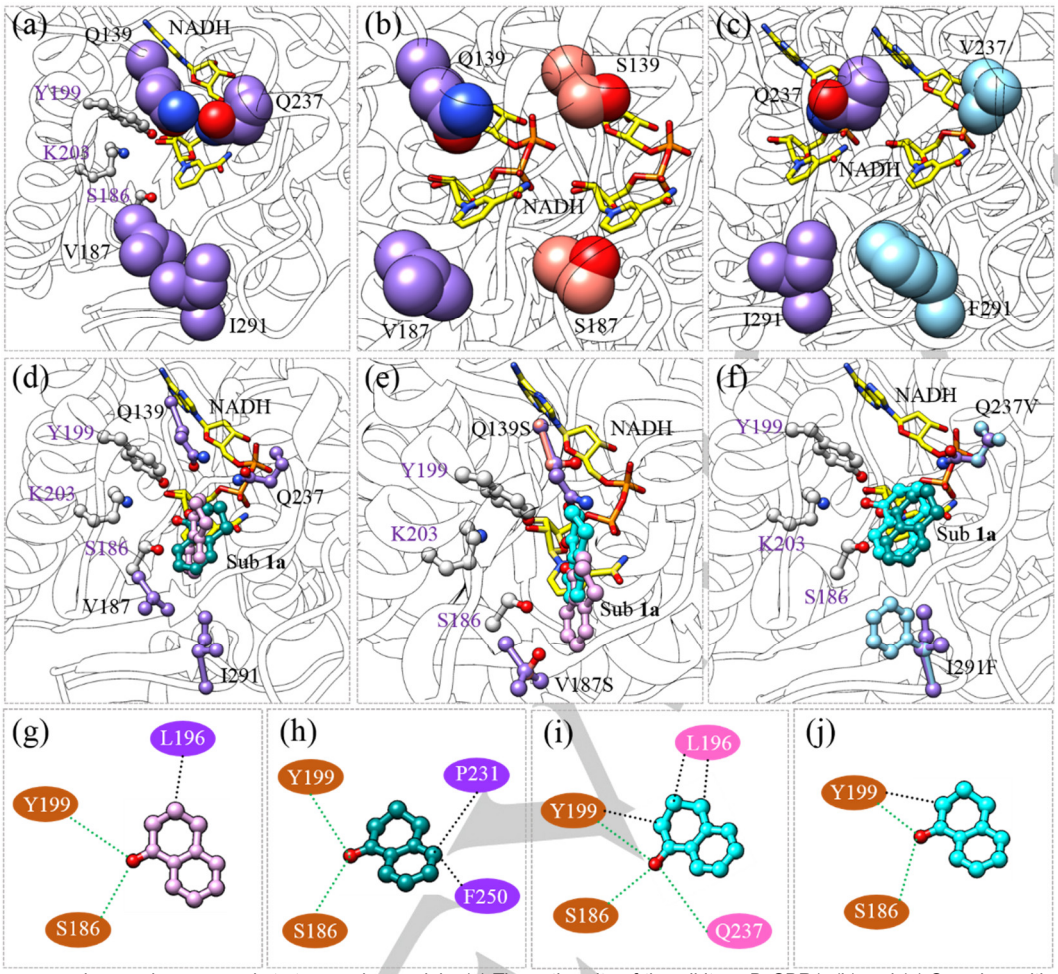

Figure 2. Structure comparison and enzyme-substrate complex models. (a) The active site of the wildtype BaSDR1; (b) and (e) Superimposition of the wildtype BaSDR1 and the variant Q139S/V253S complex models; (c) and (f) Superimposition of the wildtype BaSDR1 and the variant Q237V/I291F complex models; (d) The complex models of the wildtype BaSDR1 and substrate **1a**; (g) and (h) The interactions between the wildtype BaSDR1 and substrate **1a**; (i) The interactions between the variant Q139S/V253S and substrate **1a**; (j) The interactions between the variant Q237V/I291F and substrate **1a**. The Ser186-Tyr199-Lys203 catalytic triad is highlighted in light purple. The specific residues are indicated by labels. Green dash lines, hydrogen bonds; Black dash line, hydrophobic interactions.

double-mutation variants. The proposed catalytic mechanism of the carbonyl reductase suggests that the hydrogen atoms of the C_4 atom of NADH nicotinamide ring and the tyrosine hydroxyl were respectively transferred to the carbon atom and oxygen atom of the substrate carbonyl group during the reaction.[18] Shortening of those distances in the mutants facilitated the hydride transfer from Tyr199 and NADH to the substrates, and thus, the engineered enzyme-mediated asymmetric reduction proceeded more rapidly.[19]

The primary causes for the change of the substrate position could be ascribed to the changes of the steric hindrance and hydrophobicity of the corresponding residues in the mutants. As shown in Figure 2, the residues Q139 and Q237 were located on the Y199 side of the substrate-binding pocket. The introduction of residues harboring a smaller side chain at those sites carved out a bigger space for the proximity of the substrates to the catalytic residue Y199 and consequently contributing to the enhanced catalytic activity. However, the increased catalytic activity also was observed while I291 was substituted with a relatively bulky phenylalanine. Similar results were obtained in other enzyme engineering studies.[16, 20] This is probably due to the special location of the residue I291, which located on the opposite side of the catalytic residue Y199 (Figure 2). The increased size of the residue at this site could push the substrates close to the catalytic residues, and thus, the corresponding mutants displayed improved activity. Interestingly, the enzyme activity of the mutants also increased when V187 was substituted with a serine, though this residue also located on the opposite side of Y199 and the mutation of this site did not have significant steric hindrance change as other sites (Figure 2). In this case, the proximity of substrates to the catalytic residues was probably driven by the change of the residue hydrophobicity at this site. The aromatic ring of the substrates oriented toward residues V187. The hydrophobic aromatic ring is preferably close to hydrophobic region of the substrate-binding pocket. However, the side chain of serine is hydrophilic. The tendency of the hydrophobic benzene ring away from the hydrophilic region become a pushing force for shortening the distance between the key functional groups of the substrates and enzymes. These results indicated that it was effective to improve the enzyme catalytic performance by adjusting the steric hindrance and hydrophobicity of the residues which affect the approach of the substrate with the catalytic active site.

Furthermore, the protein-ligand interaction profile demonstrated that the dominant binding conformations of the substrates were mainly facilitated by the hydrophobic interactions

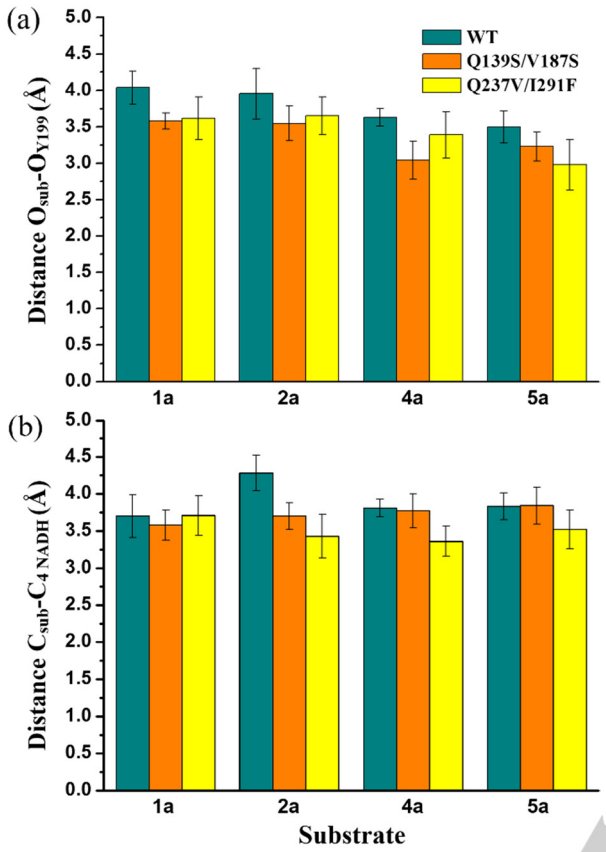

Figure 3. The distances between the key atoms in the complex models of substrates and enzymes. (a) Distance O_{sub}-O_{Y199}, the distance between the tyrosine hydroxyl and the oxygen atom of the substrate carbonyl. (b) Distance C_{sub}-C_{4NADH}, the distance between the C_4 atom of the nicotinamide ring of NADH and the carbon atom of the substrate carbonyl.

and the hydrogen bonds. The hydrophobic interactions were mainly formed between the cyclohexane ring of the substrates and the pocket-forming amino acids such as Q139, Q188, L196, Y199, P231, Q/V237, L236 and F250. The hydrogen bonds occurred more frequently between the oxygen atoms of the substrate carbonyl and the residues such as Q139 and Q239 besides the catalytic residues Y199 and S186 (Figure 2 and Figure S2-S4). It is worth noting that the introduced mutations obviously changed the enzyme-substrate interaction network in the enzyme-substrate complex models. Some of the original enzyme-substrate interactions were disrupted, while novel interactions were constructed for stabilization of the productive conformation, though the main types of enzyme-substrate interactions did not change significantly. The enzyme-substrate interactions were important driving forces for shaping substrate binding conformation and played critical roles in determining the enzyme catalytic performance.[21] Further research on the precise introduction/elimination of enzyme-substrate interactions and the evaluation of their contributions should be conducted.

Another point of concern is that the well-known trade-off between enzyme activity and stereoselectivity was observed. The mutants Q139S and Q139S/V187S exhibited significantly decreased or even reversed stereoselectivity toward substrates **1a**, **2a**, **5a** and **6a**. However, the relatively high ee values were obtained in the presence of α-tetralones **3a** and **4a** as substrates (Table 2). Further analysis showed that the size of the substrate might play an important role in determining the enzyme stereoselectivity. As shown in Scheme 1, the special position of the halogen atom on the aromatic ring of the substrates **3a** and **4a** makes their size relatively larger than those of substrates **1a**, **2a**, **5a** and **6a** in horizontal and/or vertical direction. The relative larger size restricted the binding of the substrates **3a** and **4a** to more defined conformations in the substrate-binding pocket of the mutants. It makes the mutants Q139S and Q139S/V187S retained high stereoselectivity toward the substrates **3a** and **4a**. The similar effect of substrate size on the enzyme stereoselectivity was also confirmed by the results of substrate reduction catalyzed by the wildtype enzyme and other mutants. For example, with the increase of the halogen atom size of the substrates **3a** and **4a**, an obvious increase of the stereoselectivity was observed when the mutant Q139S was utilized as catalyst. Similar results were obtained in the reduction of substrates **5a** and **6a** by the wildtype enzyme, Q139S, V187S and I291F (Table 2). It is generally accepted that the lower steric hindrance is beneficial for substrate binding and product release, resulting in a higher catalytic activity.[9, 12b, 22] However, above results indicated that the relative larger size of the substrate was beneficial for the substrates binding to the enzyme active cavity with a more specific binding mode, and further endows the corresponding asymmetric reduction with higher stereoselectivity. Excessive expansion of the substrate-binding pocket might lead to the undesired trade-off between enzyme activity and stereoselectivity. The relative size of the substrate and the substrate-binding pocket should be balanced to obtain ideal enzymes. Previous study also found that the structural flexibility of the substrates was an important factor determining the enzyme stereoselectivity.[23] Therefore, the reconstruction of the substrate-binding pocket should be performed based on a comprehensive analysis of the structural properties of the substrate to obtain enzyme with desired activity and stereoselectivity.

Potential application of the designed mutant under high substrate loading

(S)-7-Fluoro-α-tetralol is applicable to the synthesis of purinone derivatives, a class of chemical compounds with the potential for medicinal use.[5] Therefore, the mutant V187S/I291F and the corresponding fluorinated α-tetralone (**5a**) were selected as an example to test the potential of the BaSDR1 variants. Previous study found that the whole cells expressing BaSDR1 could effectively utilize glucose to recycle the cofactor and accelerate the reaction without exogenous NADH addition.[15] Thus, the recombinant *E. coli* whole cells expressing the wildtype BaSDR1 and the mutant V187S/I291F were used to catalyse the asymmetric reduction of substrate **5a** at different concentrations for evaluation of their catalytic performances.

As shown in Figure 4, in the reduction of 10 mM substrate **5a**, the mutant V187S/I291F achieved >99% conversion within 60 min. In contrast, a very low conversion (17.5%) conversion was obtained after 60 min upon using the whole cells of the wildtype enzyme, and the conversion reached only 41.5% after 300 min. The effectiveness of the mutant V187S/I291F was further evaluated with increased substrate loading. The whole cells of the mutant V187S/I291F also could efficiently catalyzed the reduction of substrate **5a** at substrate concentrations of 30 mM and 50 mM, the conversion reached >99% after 90 min and 300 min, respectively. More importantly, chiral (S)-7-Fluoro-α-tetralol was obtained with high ee value (>98%) at different substrate concentrations. These results suggested that the designed

variants could be potential tools for the synthesis of chiral α-tetralols.

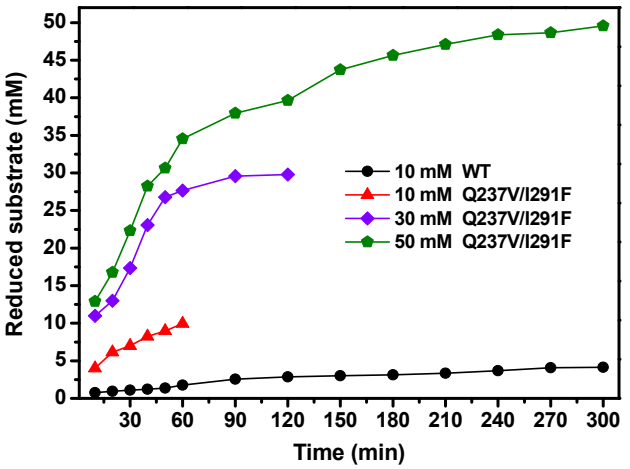

Figure 4. Asymmetric reduction of fluorinated α-tetralone **5a** by recombinant *E. coli* whole cells expressing the wildtype BaSDR1 and the variant Q237V/I291F.

Conclusion

In conclusion, the catalytic activity of the carbonyl reductase BaSDR1 toward α-tetralones was successfully improved by rational reconstruction of the substrate-binding pocket. The designed mutants exhibited potential as efficient tools for the synthesis of chiral α-tetralols. The changes of the steric hindrance and hydrophobicity of the substrate-binding pocket-forming residues turned out to be crucial factors connected to the improved activity. More notably, it was found that the substrate size played an important role in determining the stereoselectivity of enzyme-catalyzed asymmetric reduction. This was a reminder that the structural properties of the substrate should be considered as important factor in the rational design of enzymes. Precise and efficient engineering of enzyme needs to fully match the substrate and the substrate-binding pocket. This study not only provided a successful case of rational enzyme design for the asymmetric reduction of bulky-bulky ketones but also offered valuable clues for understanding the basis of the enzyme activity and stereoselectivity control.

Experimental Section

Materials

Commercial grade solvents, α-tetralone, halogenated α-tetralones and chiral alcohols used in this study were obtained from J&K Scientific Ltd. (Beijing, China) or Sigma-Aldrich (Shanghai, China). Nicotinamide adenine dinucleotide (NADH) disodium salt and isopropyl β-D-1-thiogalactopyranoside (IPTG) were obtained from Sangon, China. PrimerSTAR Max DNA Polymerase and restriction enzyme DpnI were procured from TaKaRa Biotechnology, China. Plasmid miniprep kit and polymerase chain reaction (PCR) purification kit were purchased from Transgen Biotech (Beijing, China). Primers synthesis and DNA sequencing were performed by Sangon (Shanghai, China).

Mutant construction, expression and purification

The recombinant plasmid pET30a-BaSDR1 constructed in our previous work was used as template.[15] Variants were generated by PCR-based site-directed mutagenesis and *E. coli* BL21(DE3) was used as the host cell for the overexpression of the mutants. The entire mutant gene was sequenced to exclude the undesired mutations. The expression and purification of the wildtype BaSDR1 and its mutants were conducted as previously described.[16] The protein concentrations were determined according to Bradford method employing bovine serum albumin as the standard protein.

Enzyme assay and kinetic analysis

Activity of wildtype BaSDR1 and its mutants was assayed with α-tetralones as the substrate. One unit of activity was defined as the amount of enzyme catalysing the reduction of 1.0 μmol of substrate per minute under measurement conditions. All activity assays were performed in 100 mM sodium phosphate buffer (pH 7.5) at 35 °C and 200 rpm. The standard assay mixture (1.0 mL) contained 10 mM α-tetralones, 5% (w/w) glucose, 2.0 mM NADH, 1.0 mM Co^{2+} and an appropriate amount of the purified enzyme. The reaction solutions were extracted with the same volume of ethyl acetate. The conversion and stereoselectivity were measured by a GC-9790II gas chromatography system (Wenling, China), which equipped with an FID detector and chiral column Hydrodex β-TBDAc chiral column (Macherey-Nagel, Germany, 25 m × 0.25 mm, 0.25 μm film thickness). The injector and detector temperatures were set at 250 °C. The apparent kinetic parameters of wildtype BaSDR1 and the selected mutants were determined by measuring the enzyme activity at various substrate concentrations. The Michaelis-Menten constants (K_m) were determined from plots of the initial velocity versus the substrate concentration using non-linear regression. The k_{cat} values were obtained by dividing the maximum velocity values with the enzyme concentration. All measurements were conducted in triplicate if not specified.

Molecular docking and dynamics simulation

The three-dimensional homology model of wildtype BaSDR1 was generated using the oxidoreductase YghA from *Salmonella enterica* (67% identity, PDB: 3R3S) as the template in our previous study.[15] The structure models of mutants were constructed using Swiss-PDB Viewer and refined by energy minimization. Docking studies were performed using AutoDock Vina 1.1.2 program [24] and the enzyme-substrate complexes were visualized by Chimera.[25] The binding conformation that the substrate carbonyl oxygen forms hydrogen bonds with Y199 hydroxyl and S186 hydroxyl at the same time was regarded as an effective conformation and used in the calculation of the average distances. Molecular dynamics simulation was performed as previously described.[26] The conformation of each simulation and the binding free energy of each complex were analysed by the ptraj program and mmpbsa program in AMBER package,[27] respectively.

Asymmetric reduction of 7-fluoro-α-tetralone by recombinant whole-cell

The asymmetric reduction of 7-fluoro-α-tetralone by recombinant whole-cell was studied with substrate concentrations ranging from 10 mM to 50 mM. The reaction mixture contained 0.4 g wet resting cells, 5% (w/w) glucose, 1.0 mM Co^{2+}, Na_2HPO_4-NaH_2PO_4 buffer (100 mM, pH 7.5) in a total volume of 10 ml. The reactions were carried out at 35 °C with shaking at 220 rpm. The reaction medium was sampled regularly and extracted with ethyl acetate. The organic layer was dried over anhydrous Na_2SO_4 and analysed by chiral gas chromatography.

Acknowledgements

The authors greatly acknowledge the financial support from the Natural Science Basic Research Plan in Shaanxi Province of China (2020JQ-145), the Postdoctoral Research Project of Shaanxi Province (2018BSHQYXMZZ27), the National Natural Science Foundation of China (31700700 and 31971315), the Science, Technology and Innovation Commission of Shenzhen Municipality (JCYJ20170815154418207).

Keywords: Protein engineering • Chirality • Carbonyl reductase • α-Tetralols • Asymmetric reduction

[1] T. Yasuyuki, S. Daisuke, S. Toshiaki, K. Taku, N. Yasuki, A. Nobumasa, *WO2012124825A1*, **2012**.

[2] M. L. R. Heffernan, L. W. Hardy, S. P. Brown, L. W. Herman, *US20190194163A1*, **2019**.

[3] N. Masakazu, M. Masanori, H. Tokushi, O. Shin-Ichiro, H. Hideki, T. Koji, *EP2128154A1*, **2009**.

[4] G. Wang, C. Zheng, G. Zhao, *Tetrahedron: Asymmetry* **2006**, *17*, 2074-2081.

[5] C. Kingsbury, M. Ohlmeyer, V. M. Paradkar, H. Park, J. Quintero, Y. Shao, *WO2009048474A1*, **2009**.

[6] a) J. C. Mayr, J. H. Grosch, L. Hartmann, L. F. M. Rosa, A. C. Spiess, F. Harnisch, *ChemSusChem* **2019**, *12*, 1631-1634; b) C. Aguirre-Pranzoni, R. D. Tosso, F. R. Bisogno, M. Kurina-Sanz, A. A. Orden, *Process Biochem.* **2019**, *79*, 114-117.

[7] a) S. M. Husain, A. Präg, A. Linnenbrink, A. Bechthold, M. Meller, *ChemBioChem* **2020**, *21*, 780-784; b) S. A. Serapian, M. W. van der Kamp, *ACS Catal.* **2019**, *9*, 2381-2394; c) R. Patil, L. Banoth, A. Singh, Y. Chisti, U. C. Banerjee, *Biocatal. Biotransfor.* **2013**, *31*, 123-131; d) T. Janeczko, A. Panek, A. Świzdor, J. Dmochowska-Gładysz, E. Kostrzewa-Susłow, *Curr. Microbiol.* **2012**, *65*, 189-194; e) V. Pace, Á. C. Cabrera, V. Ferrario, J. V. Sinisterra, C. Ebert, L. Gardossi, P. Braiuca, A. R. Alcántara, *J. Mol. Catal. B: Enzym.* **2011**, *70*, 23-31; f) A. Świzdor, T. Janeczko, J. Dmochowska-Gładysz, *J. Ind. Microbiol. Biot.* **2010**, *37*, 1121-1130; g) A. Pennacchio, B. Pucci, F. Secundo, F. La Cara, M. Rossi, C. A. Raia, *Appl. Environ. Microb.* **2008**, *74*, 3949-3958.

[8] a) K. Chen, F. H. Arnold, *Nature Catal.* **2020**, *3*, 203-213; b) A. Z. Khan, M. Bilal, T. Rasheed, H. M. N. Iqbal, *Chinese J. CATAL.* **2018**, *39*, 1861-1868.

[9] D. Wang, H. Li, S. Xia, Y. Xue, Y. Zheng, *Catal. Sci. Technol.* **2019**, *9*, 1961-1969.

[10] a) F. Xue, L. Zhang, Q. Xu, *Appl. Microbiol. Biotechnol.* **2020**, *104*, 2067-2077; b) K. Wu, Z. Yang, X. Meng, R. Chen, J. Huang, L. Shao, *Catal. Sci. Technol.* **2020**, *10*, 1650-1660.

[11] X. Gong, Z. Qin, F. Li, B. Zeng, G. Zheng, J. Xu, *ACS Catal.* **2019**, *9*, 147-153.

[12] a) Y. Nie, S. Wang, Y. Xu, S. Luo, Y. L. Zhao, R. Xiao, G. T. Montelione, J. F. Hunt, T. Szyperski, *ACS Catal.* **2018**, *8*, 5145-5152; b) M. M. Musa, O. Bsharat, I. Karume, C. Vieille, M. Takahashi, S. M. Hamdan, *Eur. J. Org. Chem.* **2018**, *2018*, 798-805.

[13] a) J. Zhou, G. Xu, Y. Ni, *ACS Catalysis* **2020**, *10*, 10954-10966; b) B. Su, Z. Shao, A. Li, M. Naeem, J. Lin, L. Ye, H. Yu, *ACS Catal.* **2020**, *10*, 864-876; c) G. Xu, Y. Wang, M. Tang, J. Zhou, J. Zhao, R. Han, Y. Ni, *ACS Catal.* **2018**, *8*, 8336-8345; d) O. Bsharat, M. M. Musa, C. Vieille, S. A. Oladepo, M. Takahashi, S. M. Hamdan, *ChemCatChem* **2017**, *9*, 1487-1493.

[14] E. L. Noey, N. Tibrewal, G. Jiménez-Osés, S. Osuna, J. Park, C. M. Bond, D. Cascio, J. Liang, X. Zhang, G. W. Huisman, Y. Tang, K. N. Houk, *P. Natl. Acad. Sci. USA* **2015**, *112*, E7065-E7072.

[15] A. Li, Q. Yuchi, X. Li, W. Pang, B. Li, F. Xue, L. Zhang, *Int. J. Biol. Macromol.* **2019**, *138*, 781-790.

[16] A. Li, X. Li, W. Pang, Q. Tian, T. Wang, L. Zhang, *Catal. Sci. Technol.* **2020**, *10*, 2462-2472.

[17] E. Hamnevik, D. Maurer, T. R. Enugala, T. Chu, R. Lofgren, D. Dobritzsch, M. Widersten, *Biochemistry* **2018**, *57*, 1059-1062.

[18] C. Filling, K. D. Berndt, J. Benach, S. Knapp, T. Prozorovski, E. Nordling, R. Ladenstein, H. Jornvall, U. Oppermann, *J. Biol. Chem.* **2002**, *277*, 25677-25684.

[19] X. Luo, Y. Wang, W. Shen, Y. Zheng, *J. Biotechnol.* **2016**, *224*, 20-26.

[20] a) X. L. Tang, J. Q. Jin, Z. M. Wu, L. Q. Jin, R. C. Zheng, Y. G. Zheng, *Appl. Environ. Microbiol.* **2019**, *85*, e02471-02418; b) N. Chen, Y. Chen, Y. Tang, Q. Zhao, C. Liu, W. Niu, P. Huang, F. Yu, Z. Yang, G. Ding, *Process Biochem.* **2019**, *85*, 78-83.

[21] a) Y. Wang, B. Zhang, J. Zhu, C. Yang, Y. Guo, C. Liu, F. Liu, H. Huang, S. Zhao, Y. Liang, R. Jiao, R. Tan, H. Ge, *J. Am. Chem. Soc.* **2018**, *140*, 10909-10914; b) A. Su, T. Tyrikos-Ergas, A. N. Shirke, Y. Zou, A. L. Dooley, I. V. Pavlidis, R. A. Gross, *ACS Catal.* **2018**, *8*, 7944-7951.

[22] F. Chen, G. Zheng, L. Liu, H. Li, Q. Chen, F. Li, C. Li, J. Xu, *ACS Catal.* **2018**, *8*, 2622-2628.

[23] A. Li, T. Wang, Q. Tian, X. Yang, D. Yin, Y. Qin, L. Zhang, *Chem-Eur. J.* **2021**, *27*, 6283-6294.

[24] O. Trott, A. J. Olson, *J. Comput. Chem.* **2010**, *31*, 455-461.

[25] E. F. Pettersen, T. D. Goddard, C. C. Huang, G. S. Couch, D. M. Greenblatt, E. C. Meng, T. E. Ferrin, *J. Comput. Chem.* **2004**, *25*, 1605-1612.

[26] J. Gu, H. Yu, *J. Biomol. Struct. Dyn.* **2012**, *30*, 585-593.

[27] D. A. Case, T. E. Cheatham, 3rd, T. Darden, H. Gohlke, R. Luo, K. M. Merz, Jr., A. Onufriev, C. Simmerling, B. Wang, R. J. Woods, *J. Comput. Chem.* **2005**, *26*, 1668-1688.

Entry for the Table of Contents

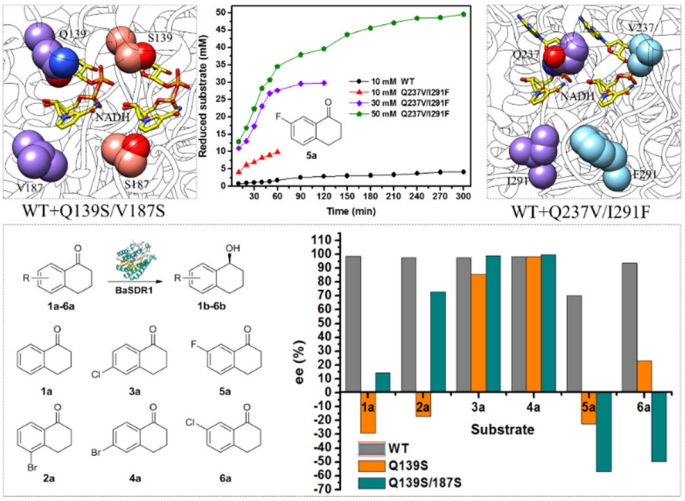

The activity of carbonyl reductase BaSDR1 toward α-tetralones, a class of bulky-bulky ketones, was successfully improved by rational design. The relative larger size of the substrates turned out to be crucial factor connected to the higher enzyme stereoselectivity.